

# Some physicochemical studies on organic eutectics and inter-molecular compounds

U. S. Rai<sup>1</sup> · Manjeet Singh<sup>1</sup> · R. N. Rai<sup>1</sup>

Received: 9 March 2017 / Accepted: 26 April 2017 / Published online: 8 May 2017  
© Akadémiai Kiadó, Budapest, Hungary 2017

**Abstract** Phase diagrams of *o*-phenylenediamine (OPDA)–*N,N*-dimethylaminobenzaldehyde (DMAB) and salicylamide (SAM)–*m*-nitro benzoic acid (NBA) systems, determined by the thaw-melt method, show the formation of two eutectics and one inter-molecular compound (IMC) in each case. These inter-molecular compounds were synthesized by the solvent-free method involving thermally initiated molten state reactions. Their characterization by the IR and the <sup>1</sup>H NMR techniques suggest the formation of a new compound. Absorption spectrum of IMC of OPDA–DMAB system shows band at 245 nm due to the  $\pi \rightarrow \pi^*$  transition and another broad band observed from 280 to 440 nm is attributed to the  $n \rightarrow \pi^*$  transition. Their IMC shows fluorescence at 388 nm with a Stokes shift (93 nm) and quantum efficiency (0.0032) upon excitation at 350 nm in ethyl alcohol. Emission and absorption were observed in case of SAM–NBA system too. While the values of enthalpy and entropy of fusion of inter-molecular compound in case of OPDA–DMAB are 23.58 kJ mol<sup>-1</sup> and 57.20 J mol<sup>-1</sup>, respectively, in the case of SAM–NBA system the corresponding values are 69.50 kJ mol<sup>-1</sup> and 170.00 J mol<sup>-1</sup>. The values of interfacial energy in case of OPDA–DMAB and SAM–NBA inter-molecular compounds are  $37.84 \times 10^{-3}$  and  $40.39 \times 10^{-3}$  J m<sup>-2</sup>, respectively.

**Keywords** Organic eutectics · Isothermal solid–liquid equilibria · Enthalpy of fusion · Green synthesis of inter-molecular compounds · Excess thermodynamic functions

✉ U. S. Rai  
usrai\_bh@yahoo.co.in

<sup>1</sup> Department of Chemistry and Centre of Advanced Study,  
Institute of Science, Banaras Hindu University,  
Varanasi 221005, India

## Introduction

With a view to cater the needs of modern civilization, the current age of science and technology demands advanced functional materials with specific properties at low cost. Materials science and engineering, in general, and crystal engineering, in particular, play a very important role although selection of a suitable material for a specific purpose is a very complicated task. However, one can simplify the choice if the details of materials about operating parameters, manufacturing processes, functional requirements and cost considerations are known. Although metallic systems [1–6] are capable of producing materials of desired specifications, their frequent preparations and uses are difficult because of high transformation temperature, difficulties involved in purification, opacity, high-density-driven convection effects and limited choice of materials. During the past few decades binary metal eutectics, monotectics and intermetallic compounds are being used for various purposes. However, binary organic systems [7–12] have gained potential importance for physicochemical investigations due to low transformation temperature, ease of purification, transparency, wider choice of materials, and minimized convection effect due to closeness in the values of the density of organic compounds. In addition, the excellent resistance to corrosion, ease of fabrication into desired shape and size, fine luster, light weight, strength, and rigidity have established the organic polymeric materials a suitable replacement of metals. Organic materials have also been reported for various electronic and optoelectronic applications such as transistor, conductor, light-emitting diode, liquid crystal display, and nonlinear optical materials. Organic molecules are widely explored to engineer the molecules for ferromagnetic materials, optical sensor, and supra-molecular device applications [13–15].

With a view to develop some binary organic materials, *o*-phenylenediamine (OPDA)–*N,N*-dimethylaminobenzaldehyde (DMAB) and salicylamide (SAM)–*m*-nitro benzoic acid (NBA) systems were chosen, and their phase diagrams were determined to know the melting temperature and composition of eutectics and inter-molecular compounds. They were synthesized by the thermally initiated molten state reaction and characterized by X-ray diffraction and thermal and optical methods. Their properties were also studied to assess their optical absorption and emission.

## Experimental

### Materials and their purification

Starting compounds, namely OPDA, DMAB, SAM, and NBA, were purchased from Sigma-Aldrich (Germany). While OPDA and NBA were purified by recrystallization in methanol, those of DMAB and SAM were purified by ethanol and deionized water, respectively. The purity of each of the materials was ascertained by the determination of their melting temperatures which were found to be very close to their literature values [16]. The melting temperatures of OPDA, DMAB, SAM, and NBA were found to be 103.0, 73.0, 140.0, and 142.0 °C, respectively.

### Phase diagram

The phase diagrams of DMAB–OPDA and SAM–NBA systems were determined by the thaw-melt method by taking appropriate amount of each of the compounds in the entire range of compositions by weighing required amount of materials in a test tube using a digital balance (Denver SI-234, Germany) of accuracy  $\pm 0.0002$  g. After sealing the mouth of each test tube these mixtures were homogenized by repeating the process of melting the mixture followed by chilling in ice-cold water. The process of melting and chilling was repeated five times to ensure proper homogenization. The melting points of these mixtures were determined using Toshniwal melting point apparatus attached with a thermometer with accuracy of  $\pm 0.5$  °C [17]. The phase diagram of a system was determined by plotting a graph between mole fraction of compound on X-axis and their melting points on Y-axis.

### Spectroscopic and optical characterizations

Infrared spectra of the pure components and their inter-molecular compounds were recorded at 300 K in the region 4000–400  $\text{cm}^{-1}$  using a Perkin Elmer FTIR Spectrum 1000 infrared spectrometer. The NMR spectra were recorded in

$\text{CDCl}_3$  by JOEL 300 MHz Spectrometer. The absorption spectra of the inter-molecular compounds as well as parent components were studied using UV/Vis/NIR (JASCO model V-670) spectrometer from 190 to 1200 nm. Fluorescence spectra were recorded on a Varian Cary Eclipse Fluorescence spectrophotometer using pyrene as reference at room temperature.

### Enthalpy of fusion

The values of heat of fusion of parent components, eutectics, and inter-molecular compounds were determined by the differential scanning calorimeter (Mettler DSC-4000 system). Indium and zinc samples were used to calibrate the DSC unit. The amount of test sample and heating rate were about 7 mg and 5 °C  $\text{min}^{-1}$ , respectively.

### X-ray diffraction

Powder X-ray diffraction of the pure components, their eutectics, and their inter-molecular compounds were recorded by Rigaku D/Max-2500/PC X-ray diffraction unit with Cu  $K\alpha$  radiation ( $\lambda = 1.5418$  Å). The powder samples were scanned from 10° to 70° with scanning rate 4°  $\text{min}^{-1}$ .

## Results and discussion

### Phase diagram study

In the phase diagram of DMAB–OPDA system (Fig. 1), the melting points of pure compounds, DMAB and OPDA, are represented in the extreme left and right sides of the

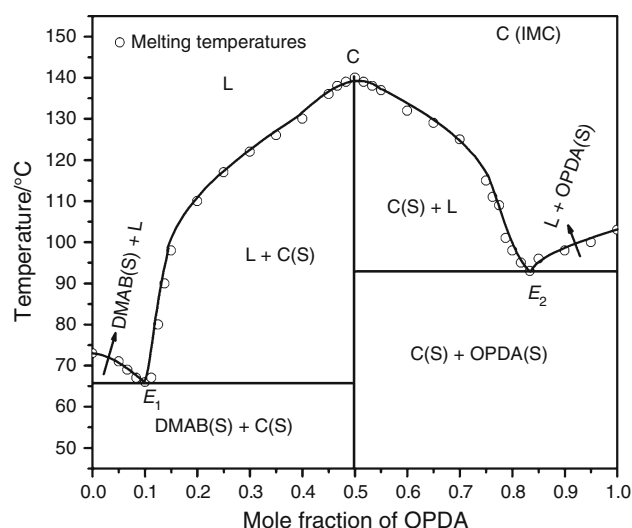


**Fig. 1** Phase diagram of DMAB and OPDA

diagram at 73.0 and 103.0 °C, respectively. The numerical values of mole fraction of different compositions were reported at X-axis and their melting temperatures were recorded on the Y-axis of the diagram. The melting point of DMAB decreases with addition of OPDA up to  $E_1$  (mp = 66.0 °C, 0.100 mol fraction of OPDA), and thereafter, it increase and reaches the maximum point at C (mp = 139.0 °C) Fig. 1 where the composition of DMAB and OPDA are in 1:1 molar ratio [18]. For each eutectic, the IMC behaves as one of the parent components. The phase diagram study reveals that there are three invariant points in the DMAB–OPDA system, namely eutectic-1, IMC, and eutectic-2.

The phase diagram of the SAM–NBA system shows the formation of an 1:2 (SAM:NBA) inter-molecular compound (IMC) at point C having congruent melting point and two eutectics  $E_1$  and  $E_2$  containing 0.342 and 0.667 mol fraction of NBA, respectively. The melting points of  $E_1$ ,  $E_2$  and the inter-molecular compound are 126.0, 124.0 and 137.0 °C, respectively (Fig. 2).

### Spectroscopic studies

**DMAB:** The peaks observed at 2795, 2713, and 1662  $\text{cm}^{-1}$  in its spectrum is indicative of C=O stretching frequency of carbonyl of aldehyde groups. In  $^1\text{H}$  NMR spectrum of DMAB peaks appear at  $\delta = 9.87$  ppm (1H s), 7.63 ppm (2H d), 6.78 ppm (2H d) and 2.85 ppm (6H s).

**OPDA:** The peaks observed at 3386 and 3364  $\text{cm}^{-1}$  are due to  $-\text{NH}_2$  group, which are due to the characteristic symmetric and asymmetric  $-\text{N}-\text{H}$  stretching vibrations. The band observed at 1609  $\text{cm}^{-1}$  is due to the  $-\text{N}-\text{H}$  wagging. The  $^1\text{H}$  NMR spectrum of OPDA shows peaks at

$\delta = 5.04$  ppm (4H s), 7.14 ppm (1H s), 6.47 ppm (1H d) and 7.30 ppm (1H d).

**Inter-Molecular Compound:** The peaks observed at 3466 and 3366  $\text{cm}^{-1}$  are due to cyclic secondary amine ( $-\text{NH}-$ ) group, which are due to the characteristic symmetric and asymmetric  $-\text{N}-\text{H}$  stretching vibrations. The band observed at 1606  $\text{cm}^{-1}$  is due to the  $-\text{N}-\text{H}$  wagging. In the  $^1\text{H}$  NMR spectrum of the complex, the peak for  $-\text{NH}_2$  proton of OPDA (5.04 ppm) is absent. Instead, a new peak in  $^1\text{H}$  NMR at 5.023 ppm is present due to ( $-\text{NH}$ ) proton [19] suggesting thereby the formation of a new compound.

FTIR of the synthesized inter-molecular compound is different from those of the parent components. The peaks observed at 3460, 3360, 3085  $\text{cm}^{-1}$  in the spectrum of the IMC of SAM-NBA system are due to stretching frequency of  $-\text{O}-\text{H}$  of carboxylic group of SAM and NBA, respectively, whereas the peaks observed at 1738 and 1566  $\text{cm}^{-1}$  are due to the C=O stretching frequency of carboxylic group of the NBA and SAM, respectively. The peaks observed at 1651, 1623 and 1594  $\text{cm}^{-1}$  in the spectrum are indicative of aromatic  $-\text{C}=\text{C}-$  stretching frequencies of IMC and peaks at 1530, 1491  $\text{cm}^{-1}$  in spectrum are due to asymmetrical and symmetrical stretching frequency of nitro group. It can be inferred from the spectroscopic data on DMAB–OPDA and SAM–NBA systems that their inter-molecular compounds are new compounds.

### Thermal studies

#### Enthalpy of fusion

The DSC plots of the parent components, the eutectics and the IMC for OPDA–DMAB and SAM–NBA systems are

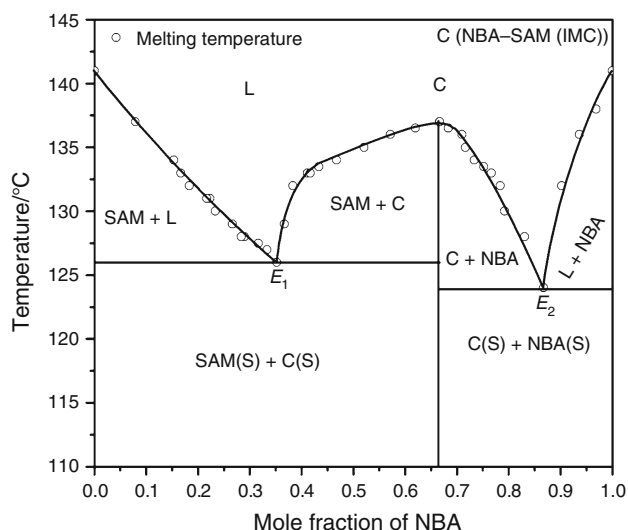


**Fig. 2** Phase diagram of SAM and NBA

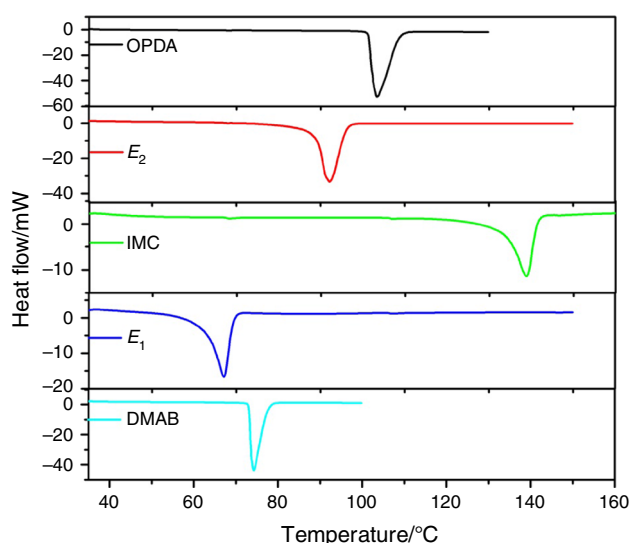


**Fig. 3** DSC plots of DMAB, OPDA, their eutectics, and inter-molecular compound

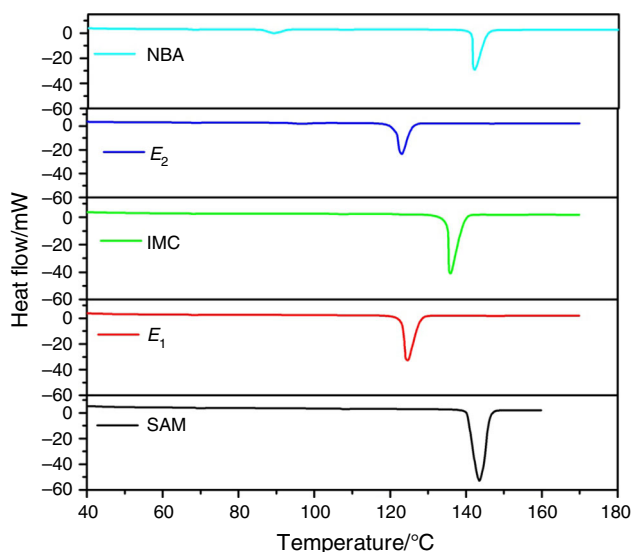


**Fig. 4** DSC plots of SAM, NBA, their eutectics, and inter-molecular compound

given in Figs. 3 and 4, respectively, and the values of their enthalpy of fusion, determined by the DSC method, are reported in Table 1. For the purpose of comparison, the values of enthalpy of fusion of eutectics and IMC, calculated by the mixture law [20], are also reported in the same Table 1. The value of enthalpy of mixing which is the difference between the experimentally determined and the

calculated values of the enthalpy of fusion is also given in Table 1. As such, three types of structures are suggested [21]: quasi-eutectic for  $\Delta_{\text{mix}}H > 0$ , clustering of molecules for  $\Delta_{\text{mix}}H < 0$ , and molecular solution for  $\Delta_{\text{mix}}H = 0$ . The highly negative value of enthalpy of mixing in cases of  $E_1$  of DMAB–OPDA system and  $E_2$  of SAM–NBA system suggests that there is strong associative interaction in the molecules of eutectic melt and their respective inter-molecular compounds [22] and in cases of  $E_2$  of DMAB–OPDA and  $E_1$  of SAM–NBA system positive value suggests that there is quasi-eutectic formation. When a melt is cooled below its melting temperature, it does not solidify spontaneously because, under equilibrium condition, the melt contains number of clusters of molecules of different sizes. As long as the clusters are well below the critical size [23], they cannot grow to form crystals, and therefore, no solid would result. During growth, the radius of critical nucleus is influenced by under cooling as well as the interfacial energy of the surface involved. However, the interfacial energy ( $\sigma$ ) is given by

$$\sigma = \frac{C \cdot \Delta_{\text{fus}}H}{(N_A)^{1/3} (V_m)^{2/3}} \quad (1)$$

where  $N_A$  is the Avogadro number,  $V_m$  is the molar volume, and parameter  $C$  lies in the range 0.30–0.35. However, to compute the interfacial energy of the eutectic, the mixture law was used. The calculated values of interfacial

**Table 1** Enthalpy of fusion, heat of mixing, entropy of fusion, roughness parameters, and interfacial energy of pure components, their eutectics, and IMCs of the both systems

S.N.	Materials	Enthalpy of fusion/ $\text{kJ mol}^{-1}$	Heat of Mixing/ $\text{kJ mol}^{-1}$	Entropy of fusion/ $\text{J mol}^{-1} \text{K}^{-1}$	Roughness parameter	Interfacial energy $\times 10^{-3}/\text{erg cm}^{-2}$
<i>OPDA–DMAB system</i>						
1.	DMAB	20.03		57.70	6.94	31.45
2.	OPDA	23.75		63.20	7.60	44.24
3.	Eutectic 1 (Exp.)	17.59	−3.15	51.70	6.22	32.73
	(Cal.)	20.74				
4.	Eutectic 2 (Exp.)	25.46	1.77	69.80	8.40	39.98
	(Cal.)	23.69				
5.	IMC (Exp.)	23.58	1.68	57.20	6.88	37.84
	(Cal.)	21.90				
<i>SAM–NBA system</i>						
6.	SAM	25.55		61.70	7.42	48.16
7.	NBA	20.49		49.40	5.94	36.51
8.	Eutectic 1 (Exp.)	52.19	3.41	131.10	15.77	44.05
	(Cal.)	48.79				
9.	Eutectic 2 (Exp.)	34.81	−5.24	87.90	10.57	38.06
	(Cal.)	40.05				
10.	IMC (Exp.)	69.52	47.34	170.00	20.45	40.39
	(Cal.)	22.18				

energy are also reported in Table 1. It is well known that decrease in free energy favors the formation of nucleus, while an increase in interfacial energy destabilizes its formation. In case of OPDA–DMAB system, the value of interfacial energy is the maximum in case of OPDA, and it is the minimum in DMAB, while in case of  $E_1$ ,  $E_2$ , and IMC the values are in between these two limits. This suggests that the role of interfacial energy is the maximum in DMAB, and it is the minimum in OPDA in destabilizing the formation of nucleus which is the first step in the formation of a crystal. Similarly the value of interfacial energy being maximum in the case of SAM and minimum in NBA suggests that it is more influential in SAM in comparison with NBA in destabilizing the formation of the nucleus.

### Excess thermodynamic functions

The deviation from the ideal behavior can best be expressed in terms of excess thermodynamic functions, namely excess free energy ( $g^E$ ), excess enthalpy ( $h^E$ ), and excess entropy ( $s^E$ ), which gives more quantitative idea about the nature of molecular interactions. The excess thermodynamic functions can be calculated by using a method reported earlier [23, 24], and the calculated values are given in Table 2. The positive values of excess free energy for  $E_1$  and  $E_2$  in both systems indicate that there is strong association between like molecules DMAB–DMAB and IMC–IMC, etc. [24], and weak interactions among unlike molecules IMC–DMAB and IMC–OPDA. In case of SAM–NBA system, the interactions SAM–SAM, NBA–NBA, and IMC–IMC are higher than those of IMC–SAM and IMC–NBA interactions.

### X-ray diffraction studies

Powder X-ray diffraction patterns of parent compounds and their eutectics and the IMC in case of OPDA–DMAB and SAM–NBA systems are depicted in Figs. 5 and 6, respectively. In case of OPDA–DMAB system, it is evident from the

figure that the XRD patterns of IMC show some new peaks which could not be assigned for either of the parent components. In addition, a change in the intensity of some of the parent peaks was also observed suggesting thereby the formation of a new compound [25]. While the powder XRD pattern of the  $E_1$  shows the peaks of the IMC and OPDA that of the  $E_2$  shows the presence of X-ray peaks of the IMC and DMAB, confirming thereby that the eutectics  $E_1$  is mechanical mixture of OPDA and IMC and eutectic  $E_2$  is mechanical mixture of IMC and DMAB. For eutectics  $E_1$  and  $E_2$ , the X-ray peaks of DMAB and OPDA, respectively, could not be observed. In case of SAM–NBA system, the X-ray diffraction pattern of  $E_1$  contains almost all peaks of IMC and SAM and that  $E_2$  has all the peaks

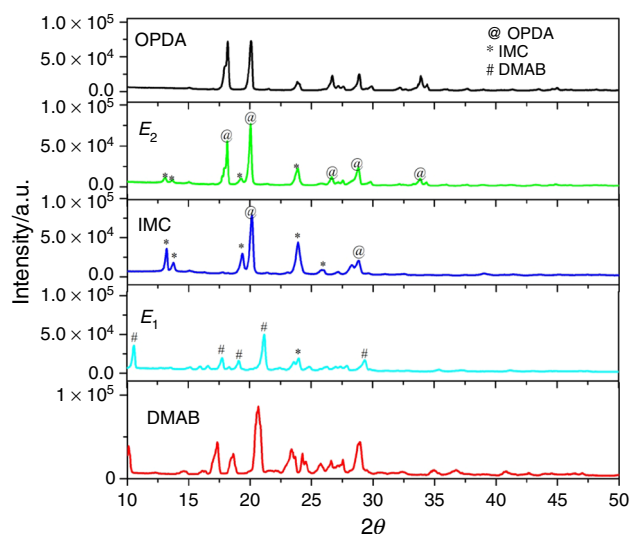


**Fig. 5** Powder X-ray diffraction pattern of DMAB, OPDA, their eutectics and IMC

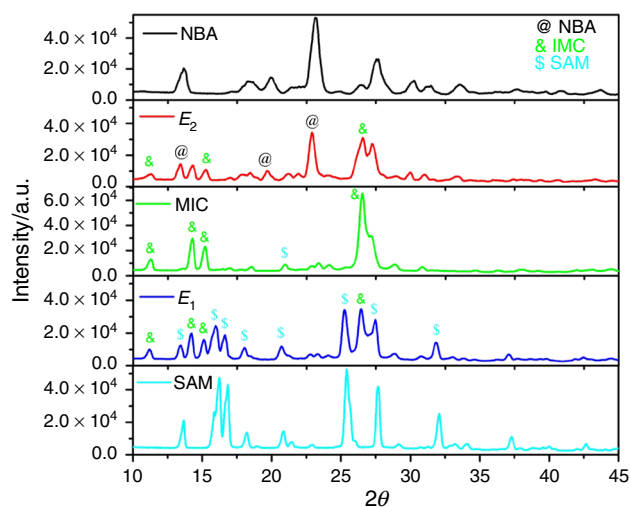


**Fig. 6** Powder X-ray diffraction pattern of SAM, NBA, their eutectics, and IMC

**Table 2** Excess thermodynamic functions of eutectics of the both systems

S. no.	Systems	$g^E/\text{kJ mol}^{-1}$	$h^E/\text{kJ mol}^{-1}$	$s^E/\text{kJ mol}^{-1} \text{K}^{-1}$
<i>OPDA–DMAB system</i>				
1	Eutectic 1	0.2666	13.4554	0.0388
2	Eutectic 2	0.5723	−2.3260	0.0079
<i>SAM–NBA system</i>				
3	Eutectic 1	0.8342	−16.1987	−0.0428
4	Eutectic 2	0.7684	−19.6869	−0.0478

of IMC and NBA. In addition, in many cases there is a change in the intensity of the peaks suggesting thereby that  $E_1$  is mechanical mixture of IMC and SAM, and the  $E_2$  is mechanical mixture of IMC and NBA. The appearance of the peaks of IMC in both eutectics suggests that the IMC behaves as a parent component for both the eutectics in both systems.

### Optical study

#### UV-Vis spectra

The optical absorption spectrum of DMAB, OPDA, and the IMC recorded at room temperature in ethanol solution ( $1.0 \times 10^{-5}$  M) in the UV-visible range 200–700 nm is shown in Fig. 7. The spectrum of DMAB shows bands at 241 and 340 nm, ascribed to the  $\pi \rightarrow \pi^*$  and  $n \rightarrow \pi^*$  transitions, respectively [25]. The bands observed in the absorption spectrum of OPDA at 240 nm is attributed to the  $\pi \rightarrow \pi^*$  transition, while a band at 295 nm appears to be due to the  $n \rightarrow \pi^*$  (primary amino group) transition [26]. The redshifts for the absorption band at 245 nm of the pure components may be due to the extension of conjugation in IMC (Fig. 7). Another new broad band observed from 280 to 440 nm is attributed to the  $n \rightarrow \pi^*$  transition, which have lower wavelength as compared to OPDA maximum absorption band because in IMC there is cyclic secondary amine as compared to primary amine present in OPDA. The broad band of IMC shows dual peaks in other solvents (except alcohols) at 336 and 377 nm, and the same wavelength of maximum has been observed in the almost all selected solvents as shown in Fig. 8.

UV-Vis spectrum of NBA shows two bands, one intense peak at 210 nm due to  $n \rightarrow \sigma^*$  transition and the other

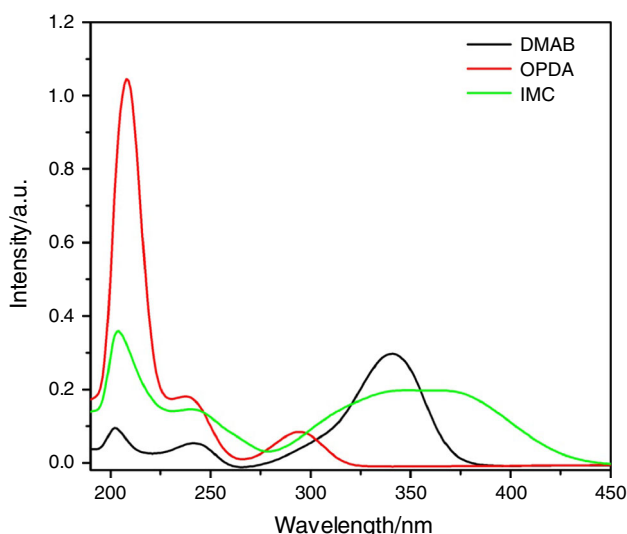


**Fig. 7** UV-Vis absorption spectra of IMC with both parent DMAB and OPDA

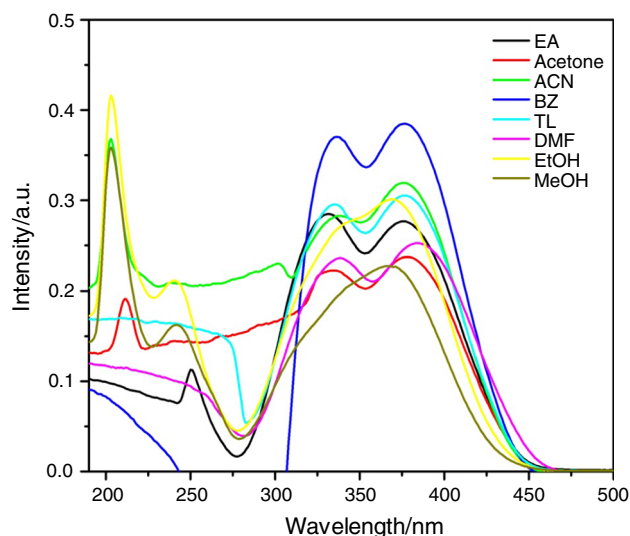


**Fig. 8** UV-Vis absorption spectra of the IMC DMAB and OPDA in different solvents

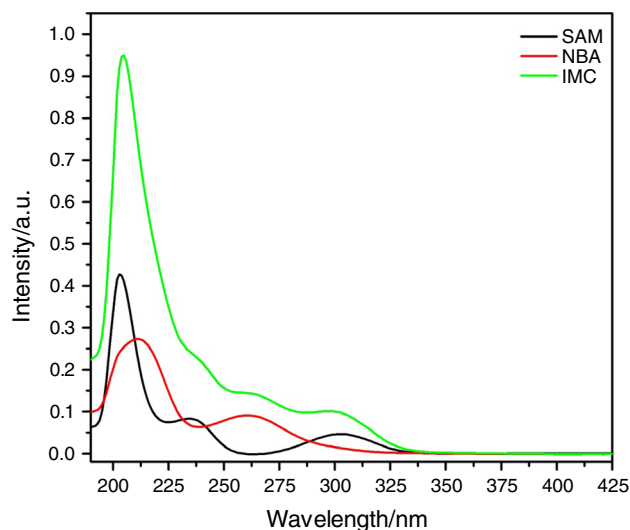


**Fig. 9** UV-Vis absorption spectra of IMC with both parent SAM and NBA

band at 262 nm comparatively of low intensity due to  $\pi \rightarrow \pi^*$  transition. SAM shows three bands at 204, 237, and 303 nm due to  $n \rightarrow \sigma^*$ ,  $\pi \rightarrow \pi^*$ , and  $n \rightarrow \pi^*$  transitions, respectively, in decreasing order of intensity. The IMC does not show any additional peak, but it retains three bands of SAM with an increase in absorption intensity (Fig. 9). It is in accordance as hyper-chromic transitions which are sensitive to hydrogen bonding.

#### Fluorescence spectra

The DMAB and OPDA do not show any noticeable fluorescence upon excitation at 340 and 295 nm, respectively. Their IMC shows fluorescence at 388 nm with a Stokes shift

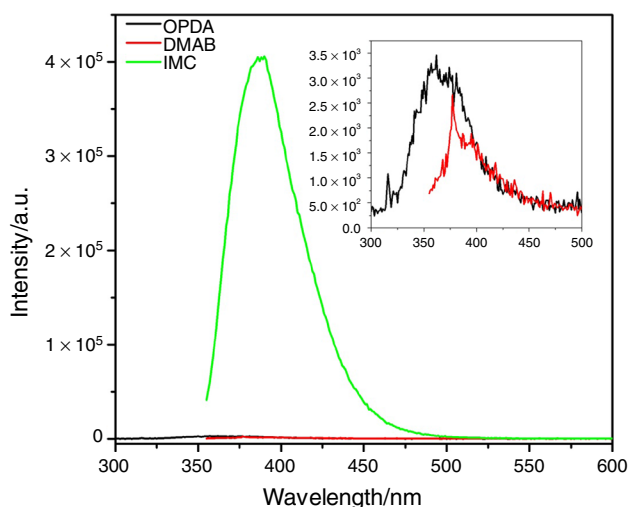


**Fig. 10** Emission spectra IMC with both parent DMAB and OPDA

**Table 3** Quantum yield and Stokes shift of the IMC of DMAB–OPDA system on excitation 318 nm in different solvents

S. no.	Solvents	Excitation wavelength	$\lambda_{\text{max}}/\text{Emi.}$	Stokes shift	Quantum Y
1.	BZ	350	381	31	0.0090
2.	TL	350	380	30	0.0123
3.	ACN	350	385	35	0.0031
4.	Acetone	350	383	33	0.0054
5.	EA	350	378	28	0.0110
6.	MeOH	350	390	40	0.0027
7.	EtOH	350	404	54	0.0130
8.	DMF	350	386	36	0.0167

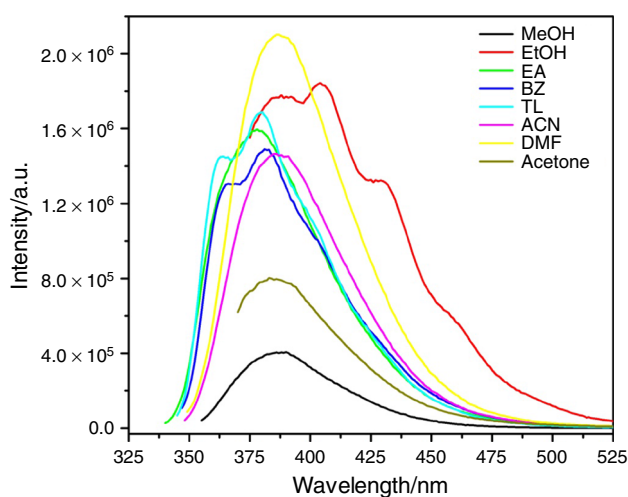


**Fig. 11** Emission spectra of the IMC of DMAB and OPDA in different solvents

(93 nm) and quantum efficiency (0.0032) upon excitation at 350 nm in ethyl alcohol Fig. 10. Quantum efficiency and Stokes shifts of the IMC in different solvents upon excitation

at 350 nm are tabulated in Table 3. The fluorescence behaviors of the inter-molecular compound may be attributed to the formation of a cyclic secondary amine moiety [27]. The fluorescence spectra of the IMC in different solvents at the same concentration are shown in Fig. 11. SAM shows emission in 325–550 nm range on  $\lambda_{\text{max}}$  excitation, while NBA does not show emission on  $\lambda_{\text{max}}$  excitation. IMC also shows emission in 325–550 nm range on  $\lambda_{\text{max}}$  (332 nm) excitation with slightly higher intensity.

## Conclusions

The phase diagram of OPDA–DMAB and SAM–NBA systems, determined by the thaw-melt method, gives two eutectics and one inter-molecular compound. While in case of OPDA–DMAB, there is formation of 1:1 IMC; in case of SAM–NBA system, it is 2:1 IMC in which concentration of NBA is twice that of SAM. While the negative values of enthalpy of mixing in E1 of OPDA–DMAB system and E2 of SAM–NBA system suggest association of molecules in their melt, the positive values of enthalpy of mixing in other two cases indicate cluster formation in their melts. The X-ray diffraction and spectral studies in both the systems suggest that eutectics are mechanical mixture of two components, while the inter-molecular compounds behave as a pure compound in both systems. The positive values of excess free energy function ( $g^E$ ) in both  $E_1$  and  $E_2$  of OPDA–DMAB and SAM–NBA systems show associative interaction among like molecules. The IMC of OPDA–DMAB system was found to emit noticeable emission at 388 nm with Stokes shift (93 nm) and quantum efficiency (0.0032), and parent components do not show such emission. In SAM–NBA system, the IMC shows more emission and absorption than those of parent components.

**Acknowledgements** We wish to express our thanks to the Head, Chemistry Department, Institute of Science, Banaras Hindu University, Varanasi, for financial support.

## References

- Chen M, Ma P. Solid–liquid equilibria of several systems containing acetic acid. *J Chem Eng Data.* 2004;49:756–9.
- Boettinger WJ, Coriell SR, Greer AL, Kerma A, Kurz W, Rappaz M, Trivedi R. Solidification microstructures: recent developments, future directions. *Acta Mater.* 2000;48:43–70.
- Rudrakshi GB, Pathak JP, Ojha SN. Processing characteristics of liquid immiscible alloys based on Al–Pb system. *Indian Foundry J.* 2002;48:17–29.
- Elliott R. Eutectic solidification processing. London: Butterworths; 1983.
- Herlach DM, Cochrane RF, Egry I, Fecht HJ, Greer AL. Containerless processing in the study of metallic melts and their solidification. *Int Mater Rev.* 1993;38:273–347.

6. Majumdar B, Chattopadhyay K. Aligned monotectic growth in unidirectionally solidified Zn-Bi alloys. *Metall Mater Trans.* 2000;31(7):1833–42.
7. Predel B. Constitution and thermodynamics of monotectic alloys—a survey. *J Phase Equilib.* 1997;18:327–37.
8. Rai US, Singh M. An overview of the progress in solidification of binary monotectics. *J Mater Chem Eng.* 2013;1:75–84.
9. Rai RN, Reddi RSB, Rai US. Developments and future directions of phase diagram, physicochemical and optical studies of binary organic complexes. 2013;59:73–111.
10. Rice JW, Fu J, Suuberg EM. Anthracene + Pyrene solid mixtures: eutectic and azeotropic character. *J Chem Eng Data.* 2010;55(9):3598–605.
11. Asta M, Beckermann C, Karma A, Kurz W, Napolitano R, Plapp M, Purdy G, Rappaz M, Trivedi R. Solidification microstructures and solid-state parallels: recent developments, future directions. *Acta Mater.* 2009;57:941–71.
12. Singh J, Singh NB. Solidification and thermodynamic parameters of binary faceted organic alloys: picric acid-resorcinol system. *J Cryst Growth.* 2015;424:14–23.
13. Parimaladevi P, Kavitha C, Srinivasan K. Investigation of the effect of liquid–liquid phase separation (LLPS) on nucleation and different growth stages of vanillin and bulk growth of defect-free single crystals from aqueous solution—a new approach. *CryStEngComm.* 2014;16:2565–9.
14. Rai RN, Ramasamy P, Lan CW. Synthesis and crystal growth of binary organic NLO material UNBA. *J Cryst Growth.* 2002;235:499–504.
15. Rai RN, Lan CW. Crystal structure and properties of new organic nonlinear optical material. *J Mater Res.* 2002;17(7):1587–91.
16. Dean JA. *Lange's handbook of chemistry.* New York: McGraw-Hill; 1985.
17. Singh M, Pandey P, Rai RN, Rai US. Solid–liquid equilibrium, thermal, and physicochemical studies on salicylamide–4-nitrophenol and 2-cyanoacetamide–4-aminoacetophenone organic eutectic systems. *J Therm Anal Calorim.* 2013;113:977–83.
18. Rai RN, Varma KBR. Phase diagram and dielectric studies of binary organic materials. *Mater Lett.* 2000;44:284–93.
19. Rajkumar M, Synthesis A. growth, structural, optical, thermal, electrical and mechanical properties of hydrogen bonded organic salt crystal: triethylammonium-3,5-dinitrosalicylate. *J Mol Struct.* 2017;1134:762–9.
20. Singh M, Rai RN, Rai US. Synthesis, crystal growth and physicochemical studies on a novel organic inter-molecular compound; 3,5-dinitrobenzoic acid and salicylamide system. *J Crystal Growth.* 2015;419:114–22.
21. Sharma KP, Rai RN. Synthesis and characterization of novel binary organic monotectic and eutectic alloys. *Thermochim Acta.* 2012;535:66–70.
22. Singh NB, Das SS, Singh NP, Agrawal Tanvi. Computer simulation, thermodynamic and microstructural studies of benzamide–benzoic acid eutectic system. *J Cryst Growth.* 2008;310:2878–84.
23. Singh M, Rai RN, Rai US. Some physicochemical and thermal studies on organic analog of a nonmetal–nonmetal monotectic alloy; 2-cyanoacetamide–4-chloronitrobenzene system. *Am J Anal Chem.* 2011;2:953–61.
24. Singh J, Singh NB. Solidification and computational analysis of o-nitroaniline–a-naphthol eutectic system. *Fluid Phase Equilib.* 2015;386:168–79.
25. Dwivedi Y, Kant S, Rai SB, Rai RN. Synthesis, physicochemical and optical characterization of novel fluorescing complex: o-phenylenediamine–Benzoin. *J Fluor.* 2011;21:1255–63.
26. Li X-G, Wang H-Y, Huang M-R. Synthesis, film-forming, and electronic properties of o-phenylenediamine copolymers displaying an uncommon tricolor. *Macromolecules.* 2007;40(5):1489–96.
27. Bani-Yaseen AD, Hammad F, Ghanem BS, Mohammad EG. On the photophysicochemical properties of selected fluoroquinolones: solvatochromic and fluorescence spectroscopy study. *J Fluoresc.* 2013;23:93–101.